American Mineralogist, Volume 79, pages 1125–1134, 1994

Kinetics of quenching of hydrous feldspathic melts: Quantification using synthetic fluid inclusions

Claudia Romano, Donald B. Dingwell, S. Michael Sterner
Bayerisches Geoinstitut, Universität Bayreuth, 95440 Bayreuth, Germany

Abstract

A microthermometric analysis of fluid inclusions preserved during the isobaric quenching of H_2O-saturated, vesicular silicate melts provides a method for the determination of the glass transition temperature of hydrous silicate melts at high pressure. The method is based on the principle that the contraction of inclusion cavities during quenching is rate-limited by the volume relaxation of the melt. Viscous relaxation of the melt ceases during cooling at the glass transition temperature. Bulk densities of the fluid inclusions whose volumes are frozen at the glass transition preserve a record of the trapping event, i.e., the glass transition temperature.

Liquid-vapor homogenization temperatures [$T_{H(L\text{-}V)}$] of the trapped inclusions are measured using a microscope heating-stage assembly. Bulk densities of H_2O present in the inclusions at $T_{H(L\text{-}V)}$ and $P_{saturation}$ are determined from literature values as are the P-T trajectories of the corresponding isochores. The intersection of an isochore with the experimental pressure during the quench yields the glass transition temperature for that particular glass composition and quench rate.

The method has been applied to seven compositions on the join albite-orthoclase. H_2O-saturated melts along this join have been rapidly and isobarically quenched at 2000 bars. The total solubilities of H_2O range from 5.12 to 6.03 ± 0.15 wt%. The glass transition temperatures of the H_2O-saturated melts range from 525 to 412 °C. The compositional dependence of the glass transition is strongly nonlinear. Melts of intermediate composition exhibit a significantly lower glass transition than either end-member. The deviation from additivity reaches a maximum of 70 °C at $Ab_{50}Or_{50}$ (molar basis).

The information on T_g can be combined with data for the properties of the quenched glasses to obtain liquid properties at hydrothermal conditions, for example, the viscosity and the thermal expansivity of the wet melts. The quantification of trapping temperatures for fluid inclusions in silicate melts also has potential applications in the study of the kinetics of melt degassing.

Introduction

Perhaps the most spectacular case of the composition dependence of melt properties results from the addition of a few weight percentages of H_2O to acidic silicate melts (Shaw, 1963). The transport properties of such melts are known to be drastically influenced by the presence of dissolved H_2O (Sabatier, 1956; Burnham, 1963; Shaw, 1963; Watson, 1981). It is clear that the dependence of these transport properties on H_2O content is a controlling factor in the physics of plutonic and subvolcanic petrogenetic processes. Another remarkable aspect of acidic silicate melts, wet or dry, is the extremely large temperature dependence of some transport properties in the temperature range corresponding to the late stages of petrogenesis. In particular, melt viscosity, and other related properties, can vary (in the range of eruption temperatures of some acidic volcanoes) by a factor of 10 over a mere 30 °C (Carron, 1969). This extreme temperature dependence at geologically relevant temperatures makes quantitative prediction of the properties of igneous melts, which are being cooled rapidly during eruption, extremely difficult. The combination of the strong H_2O-concentration dependence and the temperature dependence of the transport properties of acidic silicate melts means that one of the outstanding challenges of the prediction of melt behavior in the critical temperature range of crystallization and eruption lies in the acquisition of transport property data for hydrous silicate melts at relatively low temperatures and high viscosities. Only through a combination of high and low temperature data can a reasonable interpolation of property data over the entire temperature range of petrogenesis be made.

The limiting case of the viscous deformation of silicate

0003–004X/94/1112–1125$02.00

melts is a viscoelastic transition that expresses the glass transition in silicate melts. At this transition, many configurational changes in the structure of the liquid cease to change with further cooling. Thus, the lowest temperature directly relevant to the igneous petrogenesis of incompletely crystallized igneous rocks is that of the glass transition. This transition has important consequences not only for the rheology but also for the thermal expansivity and heat capacity of melts and magmas. It is thus apparent that knowledge of glass transition temperatures for magmas involved in eruptive processes is a prerequisite for the modeling of volcanic systems. Because the glass transition is a kinetic phenomenon, reference to its temperature must always be accompanied by explicit or implicit reference to the time scale of interest. This feature is not only of theoretical importance. Quite the contrary, the temperature-dependence of the time scale associated with the glass transition scales nearly linearly to the temperature dependence of the viscosity, whose great magnitude we have already noted above (Scherer, 1986; Dingwell and Webb, 1989). The practical consequences of a glass transition temperature that varies with time scale can be extreme. The brittle-ductile transition of a magma during eruption might be crossed repeatedly during cooling because of the successively longer time scales of deformation accompanying successively cooler deformation events, for example, in the formation of pyroclastic deposits. A magma that has behaved brittlely in the volcanic vent can behave ductilely at even lower temperature during ignimbrite compaction, as is the case for ignimbrite fiamme (Fisher and Schminke, 1984).

The chemical principles underlying the incorporation of H_2O into silicate melts, i.e., those responsible for the observed dependence of melt properties on H_2O concentration, can only be understood when the dependence of H_2O solution on temperature, pressure, H_2O concentration, and composition has been isolated. In recent years, much progress in our understanding of the solution of H_2O in silicate melts has been achieved (Stolper, 1982a, 1982b; Silver and Stolper, 1985; Eckert et al., 1987; Silver and Stolper, 1989; Kohn et al., 1989; Dingwell and Webb, 1990; Ihinger, 1991; Zhang et al., 1990; Holtz et al., 1992, 1993). This has resulted, in part, from recognizing that the majority of the now-abundant data for the speciation of H_2O in silicate glasses (Stolper, 1982a, 1982b, 1989; Silver et al., 1990; Ihinger, 1991) must be corrected to the structural state of the glass produced during the quench (i.e., correcting for the glass transition temperature: Dingwell and Webb, 1990). For this we need glass transition temperatures for experimental quenches of hydrous melts.

From the above discussion it becomes clear that an accurate understanding of the dependence of the glass transition on pressure, temperature, composition, and H_2O concentration could contribute greatly to the modeling of igneous processes and to the evaluation of experimental products. Such considerations have led us to evaluate possible methods for studying the glass transition in hydrous melts.

How is the glass transition temperature measured? Traditional studies of determination of the glass transition temperature were, for practical reasons, restricted to a very narrow interval of experimental time scale or relaxation times. Historically, interest in the glass transition was an outgrowth of processing of industrial glass. Knowledge of the annealing behavior over a relatively restricted range of time scales was all that was needed. Thus the importance of the explicit definition of the relaxation time scale remained vague. In contrast, time scales for igneous processes (Spera et al., 1981; Dingwell and Webb, 1989; Webb and Dingwell, 1990a, 1990b) and for experimental methods in mineral and melt physics (Bagdassarov et al., 1993; Webb, 1992; Webb and Dingwell, 1990a, 1990b) may span many orders of magnitude. A simple but powerful example of the latter is that of ultrasonic wave propagation in sodium disilicate melt, which generates a glass transition temperature 300 °C above that obtained by conventional means (Webb, 1992) because of the shifted time scale of the method.

As noted, the traditional methods of glass transition studies span a relatively small range of time scales. The most common measurements are dilatometric determination of the expansivity (Tool and Eichlin, 1931; Knoche et al., 1992; Webb et al., 1992) and calorimetric determination of the heat capacity (Martens et al., 1987). The application of such methods to geologically relevant melt compositions has been pursued in the past few years (Dingwell and Webb, 1989; Webb and Dingwell, 1990a, 1990b; Dingwell, 1993). The dilatometric method at 1 atm has even been applied to wet rhyolite glasses (Taniguchi, 1981), although H_2O loss is a potential problem. The calorimetric method has also been applied by Rosenhauer et al. (1979) to dry melts at high pressure. Hydrous melts at high pressure have not yet been investigated. Here we present a new method for the determination of the glass transition temperature in the high pressure, vesicular, hydrous glasses that are the common product of hydrothermal experiments in petrology. We draw attention to a number of potential pitfalls in the method and, having tested for flaws, apply the method to the system albite-orthoclase-H_2O at 2000 bars.

Method

Theory

A general outline of the principles of relaxation, the glass transition and their relationship to the cooling or quenching of silicate melts into the glassy state, has been provided in recent years (Dingwell and Webb, 1989, 1990). The use of estimated transition temperatures in predicting the structure and properties of silicate liquids from their quench glasses has also been described (Richet and Bottinga, 1984; Brandriss and Stebbins, 1988; Webb and Dingwell, 1990a, 1990b; Dingwell, 1990, 1993; My-

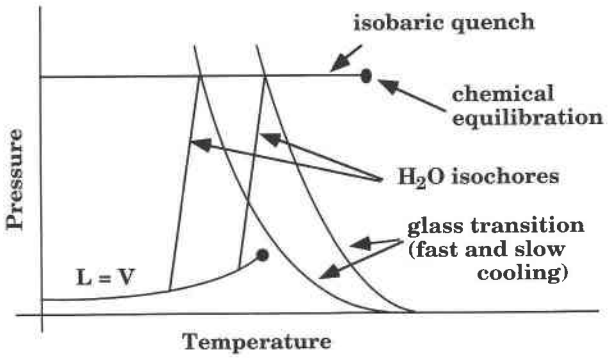

Fig. 1. A schematic illustration of the method used in the study for the determination of the glass transition temperature of hydrous silicate glasses. See text for discussion of this figure (redrawn from Dingwell, 1993).

sen and Frantz, 1992). The following discussion is restricted to those aspects of the glass transition relevant to the principle employed here.

The experimental method currently employed for the determination of T_g is illustrated schematically in Figure 1. The *P-T* trajectories of the H_2O liquid-vapor coexistence curve from some low temperature up to the critical point and of two representative isochores (lines of constant H_2O density) are as indicated. Initially, the experimental charge is allowed to dwell for a time sufficient to allow the chemical equilibration of a H_2O-saturated silicate melt at pressure and temperature. The melt contains bubbles because the viscosity of the liquid (initially a powder) is high enough to prevent the escape of vesicles during the experiment. The horizontal line extending down-temperature from the dwell point represents an isobaric quench path of the experiment. The two curves with negative slopes represent hypothetical glass transition curves corresponding to different cooling rates. The negative slopes of the curves is based on the observation that the (isothermal) viscosity of H_2O-saturated melts decreases with increasing pressure, due to increasing H_2O content.

Consider the fate of inclusions of H_2O in the vesicles of an equilibrated, H_2O-saturated silicate melt during the isobaric quenching. If one assumes that the quench is sufficiently rapid that no significant exchange of H_2O occurs between melt and fluid, then the mechanical response to the quench is a simple contraction of melt and bubbles, by volume relaxation, down to lower temperature. This viscous contraction continues with decreasing temperature until a temperature point where the exponentially increasing viscosity, reflecting a structural relaxation time for the melt, becomes too high. This point is the glass transition temperature for the cooling rate used. It is the temperature at which the structure of the equilibrium liquid most closely resembles the structure of the quenched glass: it is here that the densities of the ideally nonreacting fluid inclusions are frozen in.

TABLE 1. Analyzed anhydrous compositions and H_2O contents of glasses (wt% oxide)

Glass	SiO_2 (±1)	Al_2O_3 (±0.5)	Na_2O (±0.7)	K_2O (±0.6)	H_2O^* (±0.15)	Total
Na_{100}	68.1**	19.1	11.8		6.03	99.00
	68.7	*19.4*	*11.8*			
$Na_{90}K_{10}$	69.1	19.0	10.9	1.8	6.03	101.00
	68.3	*19.3*	*10.6*	*1.8*		
$Na_{70}K_{30}$	67.8	19.0	8.0	5.4	6.00	100.20
	67.5	*19.1*	*8.1*	*5.3*		
$Na_{50}K_{50}$	67.6	18.9	5.6	8.7	5.81	100.80
	66.7	*18.9*	*5.7*	*8.7*		
$Na_{30}K_{70}$	66.4	18.8	3.3	12.0	5.52	100.50
	65.9	*18.6*	*3.4*	*12.1*		
$Na_{10}K_{90}$	65.3	18.8	1.2	15.6	5.27	100.90
	65.1	*18.4*	*1.1*	*15.3*		
K_{100}	65.4	18.5		16.5	5.12	100.40
	64.8	*18.3*		*16.9*		

Note: nominal compositions are italicized. $Na_{100} = NaAlSi_3O_8$ (albite), $K_{100} = KAlSi_3O_8$ (orthoclase).
* Measured by Karl Fischer titration (Romano et al., in preparation).
** Compositions determined by ICP analysis.

Subsequent determination of the bulk densities of fluid inclusions trapped in the quenched glasses by measuring their liquid-vapor homogenization temperatures can then be used to define isochores (Fig. 1) that must intersect the isobaric quench path at T_g. Our tests of the method, and the results presented below, indicate that under certain conditions of experimental quench, H_2O content, and pressure, fluid inclusion analysis can be used successfully to predict the glass transition temperature.

Synthesis

The anhydrous starting glasses used in the present study were generated by the direct fusion of 100 g (decarbonated equivalent) batches of powder mixes of the alkali carbonates, SiO_2, and Al_2O_3. The powder mixes were fused in air in thin-walled 75 cm^3 Pt crucibles for approximately 2 h at 1650 °C. The products of the initial fusion were vesicular. To remove bubbles, to react fully, and to homogenize the starting glasses, the melted batches were transferred to a second furnace equipped with a high-temperature viscometer and stirred at 50 or 100 rpm for hours to days at 1650 °C. The products of these second fusions were cooled in air by removing them from the furnace, and they were sampled for dilatometry and hydration experiments by drilling cores 8 and 3 mm in diameter with H_2O-cooled diamond coring tools. Glasses so produced were analysed by ICP-AES. The results of the analyses are presented in Table 1.

Glass samples were then crushed to obtain a powder for hydrothermal experiments (grain size of the powder: 200–500 μm). One hundred mg of powder were loaded together with ~10 mg of doubly distilled H_2O in capsules formed from Pt tubing and sealed with an arc-welder. The amount of added H_2O was chosen to be about 4–5 wt% higher than the expected solubility of H_2O in these melts (on the basis of data from Romano et al., in prep-

aration). This value was chosen to be high enough to produce a large number of fluid inclusions but low enough to minimize possible changes in the anhydrous stoichiometry of the melt resulting from incongruent dissolution of silicate components in H_2O. The capsules were checked for possible leakage by testing for weight loss after drying in an oven at 100 °C for at least 1 h.

The capsules were placed in TZM vessels, pressurized to 2 kbar, and heated to 1100 °C where they were held for a time sufficient to allow the complete homogenization of H_2O dissolved in the melt by diffusion through the sample. Experiment durations ranged from 3 to 5 d. Temperature was measured with a Ni-NiCr thermocouple (accuracy ±15 °C), and the pressure was measured with a strain-gauge manometer (accuracy ±20 bars). After the high pressure–high temperature dwells, the samples were quenched in the TZM vessels by dropping the sample into the cold part of the vessel (estimated quench rate 200 °C/s). Special care was taken during the quench to maintain isobaric conditions by opening the vessel to the pressure line (2000^{+50}_{0} bars).

Fluid inclusion analysis

After quenching, the samples were crushed to millimeter-sized fragments in preparation for microthermometric investigation of the fluid inclusion, liquid-vapor, homogenization temperature. Attempts to perform heating stage analyses on the experimental glasses under 1-atm of air pressure were unsuccessful. The pressure difference (≤60 bars) between the fluid inclusions and the ambient conditions resulted in the decrepitation of inclusions and the fragmentation of entire specimens. To eliminate this problem, small inclusion-bearing glass chips were loaded along with pure H_2O in a doubly polished, fused silica tube (1–1.5 cm long, 1-mm i.d., 2-mm o.d.). The vapor pressure generated in the tube during the heating stage measurements was then equal to that in the fluid inclusions prior to homogenization. Inclusion decrepitation was thus prevented by eliminating the differential pressures across the sample.

Microthermometric measurements of phase transitions in fluid inclusions trapped in quenched glasses were performed using a petrographic microscope equipped with a slightly modified gas-flow heating and freezing stage from Fluid, Inc. (Werre et al., 1979). Because of the unusual sample geometry required by the enclosure of the glass fragments within a 2-mm o.d. silica glass tube, special procedures were employed to characterize and minimize thermal gradients within the stage over the observed range of homogenization temperatures. The glass plate on which the sample rests under normal operating conditions was replaced by a slotted Cu plate, which held the silica tube at approximately the same vertical position. Upper and lower facets were ground into the silica tube to facilitate visual observations. All T_h measurements were made with the thermocouple tip resting on the approximate center of the tube; thus the maximum distance of any measured inclusion from the thermocouple tip was <1 cm. The maximum range observed in T_h for inclusions from a single sample is 9 °C. A range of 4 °C is more typical.

The thermal gradient present during the heating experiments was determined by a temperature calibration of the stage. The temperature standards used for the calibration were powders of $KClO_4$ (ICTA certified reference material 759) and KNO_3 (Alfa Products s-89812). The temperature references were a phase transition at 299 °C in $KClO_4$ and the melting of KNO_3 at 333 °C. This calibration leads to a temperature correction for homogenization temperatures of 15 ± 6 °C. This calibration was performed with the quartz tube at dry conditions. Convection of the H_2O medium under the pressure of the liquid-vapor coexistence curve might reduce the correction. The above correction should be viewed as a maximum estimate. It has been applied to the results reported below.

Final melting temperatures of fluid inclusions in quenched glasses were observed without confinement in silica tubes. Associated uncertainties in T_m measurements are estimated at ±0.1 °C and reflect the combined effects of low-temperature thermal gradients and thermocouple calibration errors.

Prior to homogenization, several inclusions were selected from each sample, and their longest and shortest visible dimensions of several inclusions were recorded for later volume calculations. All the inclusions examined in this study homogenized to the liquid along the pure H_2O liquid + vapor (L + V) curve. No homogenization caused by fading of the meniscus or disappearance of the liquid phases was observed. The choice of the heating rate was critical. Inclusions that were heated too quickly exhibited a hysteresis due to kinetic factors, whereas inclusions that were heated too slowly exhibited an increase in the volume of the vapor phase, presumably caused by H_2O loss or inclusion deformation (see below). A heating time of about 0.1 °C/s (in the temperature range of homogenization), intermediate between the two extremes, was chosen and was kept identical for all the measurements.

Fluid composition

To estimate the glass transition temperature using our proposed method one must be able to predict accurately the phase equilibria and volumetric properties of the fluids trapped in the inclusions. An obvious prerequisite is that one knows the composition of the fluid. In the present experiments, we have modeled the behavior of the inclusion fluids after the properties of pure H_2O. This is justified because (1) we had prior knowledge of the starting composition, and (2) final melting temperatures of selected fluid inclusions were 0.0 ± 0.1 °C, thus precluding the possibility of significant dissolved solids at low temperatures, and (3) the inclusion decrepitation problem was resolved by using the silica tubes to eliminate the pressure differential, indicating that negligible amounts of expandable gases were present. The above considerations imply that the composition of the fluids trapped in the inclusions was essentially pure H_2O and that we can

TABLE 2. Microthermometric data from synthetic fluid inclusions

Composition	T_h (°C)	T_g (°C)
Na_{100}	285–289*	450–458
$Na_{90}K_{10}$	272–277	427–436
$Na_{70}K_{30}$	273–275	429–432
$Na_{50}K_{50}$	263–267	412–419
$Na_{30}K_{70}$	285–290	450–459
$Na_{10}K_{90}$	302–305	483–489
K_{100}	312–321	504–525

Note: Na_{100} = albite ($NaAlSi_3O_8$), K_{100} = orthoclase ($KAlSi_3O_8$); subscripts refer to mole percent.

* Ranges in T_h refer to ranges of measured homogenization temperature for a set of inclusions.

predict the properties of these inclusions with data from the H_2O system with high confidence. It is worth noting, however, that the successful application of the present method does not require that the fluid be pure H_2O but merely that its phase relations and volumetric properties be known.

Elastic volume corrections

The glass containing the fluid inclusions continues to contract with reducing temperature down to room temperature. All contraction below the glass transition is, however, elastic or recoverable as is the case for crystal hosts (Scherer, 1986). At the end of the isobaric quench, the glass is depressurized, at room temperature, to atmospheric pressure. The decompression is also accompanied by an elastic volume change, an expansion, of the host glass. For an accurate calculation of the glass transition temperature from the measurement of the homogenization temperature, both of these elastic volume changes must be corrected for. The relevant corrections are the expansion and compression expected between T_h and T_g and P_h and P_g, respectively. The expansivity and compressibility of hydrous glasses are not well known, but estimates for the liquid may be made, for example, from the study of Burnham and Davis (1971). We chose values of 3×10^{-5} °C^{-1} and 50 GPa for the expansivity and bulk modulus, respectively. The thermal expansion and the compression effects counteract each other, and the combined correction for expansivity and compressibility results in a maximum temperature correction of +1 °C. This correction has been applied to the results of Table 2.

Next we discuss the main assumptions and limitations involved in the fluid inclusion technique presented for the estimation of the glass transition temperature in this study. Potential sources of error in these measurements include changes in the density of the inclusions after trapping.

Inclusion stability at room temperature

Change in inclusion density might occur at room temperature, as a function of time. To evaluate this possibility, we have tested the stability of our glasses at room temperature by measuring the volume change of the vapor bubble with time in fluid inclusions chosen from various samples and synthesized under varying conditions. A significant difference in behavior was observed for similar samples synthesized using several quench rates. Figure 2 illustrates two examples of our investigation of the room-temperature stability of fluid inclusions. In general, samples quenched relatively slowly by using compressed air (200 °C/min) were relatively unstable (Fig. 2a). For these samples, the density change appears to be inversely related to the inclusion volume being quite pronounced for inclusions smaller than 50 μm and minor for inclusions having larger diameters (shaded area in Fig. 2a). Samples quenched by dropping the experimental capsule into the cold part of the vessel (200 °C/s), showed, in contrast, a high stability, and negligible density changes occurred as a function of time (~5 °C over 1 week: Fig. 2b). This relative instability of the slowly quenched glasses is somewhat unexpected. One might anticipate that thermal stresses induced during the quench would be larger at higher quench rates. This is the typical observation in glass studies. Here, the relative instability of the slowly quenched samples requires a different explanation.

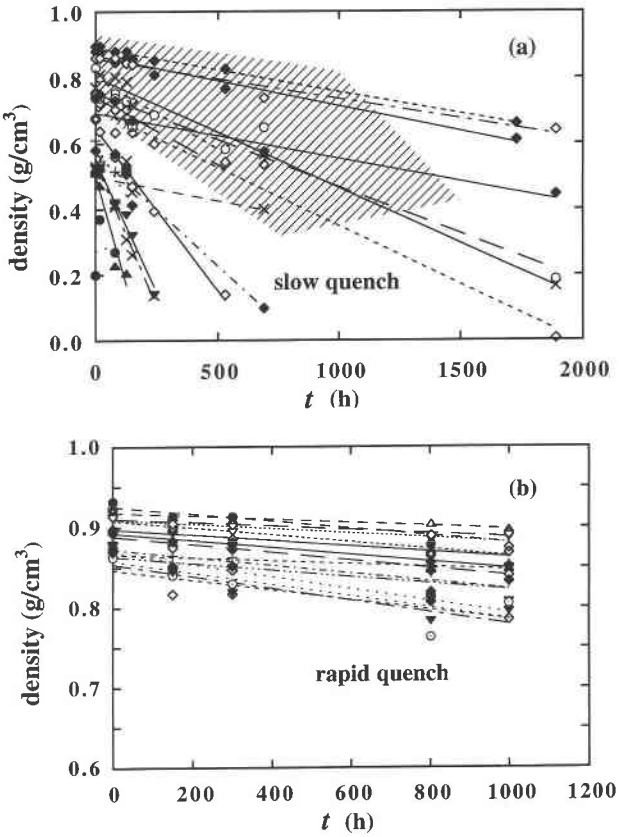

Fig. 2. Stability of fluid inclusions quenched into hydrous glasses. The slowly quenched sample (**a**) exhibits fluid inclusions that are much less stable than those in the rapidly quenched sample (**b**), which illustrates a very stable population of inclusions. See text for discussion. Examples shown are individual experiments.

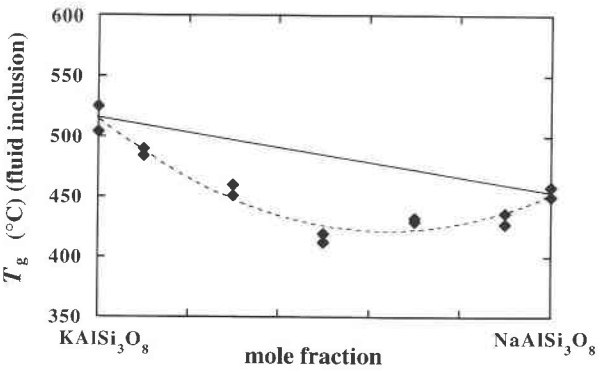

Fig. 3. Calculated glass transition temperatures of hydrous alkali feldspar melts, isobarically quenched from H_2O-saturated conditions at 1100 °C and 2 kbar, determined from the homogenization temperatures. Note the strong deviation from additivity attributed to the configurational entropy of mixing.

One possibility is that significant transport of H_2O from inclusions to glass occurs during the slower quench. Such transport could generate a H_2O-enriched (or depleted) rim around the inclusions, with the resulting possibility that differential thermal contraction between the rim and glass bulk causes thermal stresses and subsequent fracturing. The fractures could then be the source of the observed instability.

Although the cause of the quench-rate dependence of this inclusion behavior has not been determined, it has been demonstrated for the rapidly quenched samples that changes in inclusion density at room temperature are negligible for times of up to 1 week. Therefore, only rapidly quenched samples have been employed in the present study, and our fluid inclusion analyses, always performed within 2–3 d of quenching, thus reflect true quenched densities.

Stability during microthermometric analysis

Several possible mechanisms exist that could lead to the instability of inclusions during heating in the microthermometric stage. These include two mechanisms already discussed in the fluid inclusion literature: (1) changes in density due to microfractures (leading in the extreme case to decrepitation, see below) and (2) loss of H_2O through bulk or surface diffusion, as well as the additional possibility of an elastic viscous deformation of the host melt (not observed in crystals). All the above mechanisms lead to a rise in measured T_h as a function of time and overheating. Each of these mechanisms, if significant, can generate inclusions that yield reproducible but erroneously high values of T_h.

We have defined some general criteria for excluding the above phenomena: (1) constancy of the volume of the bubble before and after the first experiment (verified by optical measurements of its diameter) and (2) consistency of T_h results on subsequent, repeated, microthermometric experiments. The first of these tests demonstrates that the first heating of an inclusion does not result in significant instability before the initial T_h determination is made. The second test shows that this is also the case for the subsequent analyses. We have observed that the initial heating experiment on fluid inclusions has no measureable effect on inclusion density. Thus, significant inclusion instability below T_h, on the time scale of our microthermometric experiments, can be ruled out. Significant heating of the inclusions beyond T_h does, however, result in density decrease (i.e., instability), illustrated by a drift to higher subsequent values of T_h. This instability can, however, be prevented by the careful avoidance of significant overheating. For inclusions that have not been heated more than 5 °C above T_h, no drift in T_h determinations is observed, i.e., the inclusions behave stably.

As noted above, the extreme consequence of microfracturing is decrepitation. This violent, permanent deformation of the glass around an inclusion occurs when the differential between the internal pressure in an inclusion and the external confining pressure exceeds some threshold value. This value depends on the strength of the host material (the quenched glass) and the inclusion size. A number of studies of the decrepitation behavior of fluid inclusions in crystalline solids have been performed, but they are of questionable relevance in the present investigation because the differential pressures required to decrepitate the present samples are much lower than those reported in the literature (Naumov et al., 1966; Leroy, 1978; Swanenberg, 1980; Roedder, 1965). As an example, a pure H_2O inclusion containing liquid and a vapor bubble has an internal pressure <1 bar at 25 °C. If this pure H_2O inclusion were to homogenize at 280 °C, the vapor pressure (at that temperature) would be ~64 bars. Several fluid inclusions measured in the present study had homogenization temperatures near 280 °C when sealed together with H_2O in silica tubes to eliminate the

TABLE 3. Glass transition temperature from dilatometry

Composition	Cooling rate (°C/min)	T_g (°C)
K_{100}	x	978
K_{100}	10	976
K_{100}	1	971
$K_{90}Na_{10}$	x	939
$K_{90}Na_{10}$	10	931
$K_{90}Na_{10}$	1	924
$K_{70}Na_{30}$	x	865
$K_{70}Na_{30}$	10	855
$K_{70}Na_{30}$	1	850
$K_{50}Na_{50}$	x	820
$K_{50}Na_{50}$	x	822
$K_{50}Na_{50}$	10	818
$K_{50}Na_{50}$	1	814
$K_{30}Na_{70}$	x	806
$K_{30}Na_{70}$	10	814
$K_{30}Na_{70}$	1	814
$K_{10}Na_{90}$	x	814
$K_{10}Na_{90}$	10	815
$K_{10}Na_{90}$	1	815
Na_{100}	x	820
Na_{100}	10	824

Note: Na_{100} = $NaAlSi_3O_8$, K_{100} = $KAlSi_3O_8$; x = annealed (slow but unmeasured cooling rate).

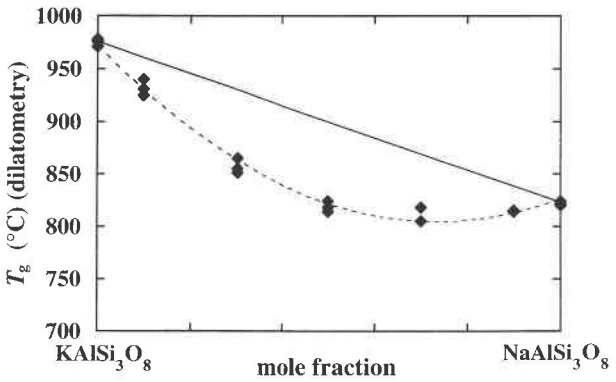

Fig. 4. The glass transition temperature of dry alkali feldspar melts quenched at 1 atm pressure. The deviation from additivity is attributed to the configurational entropy of mixing.

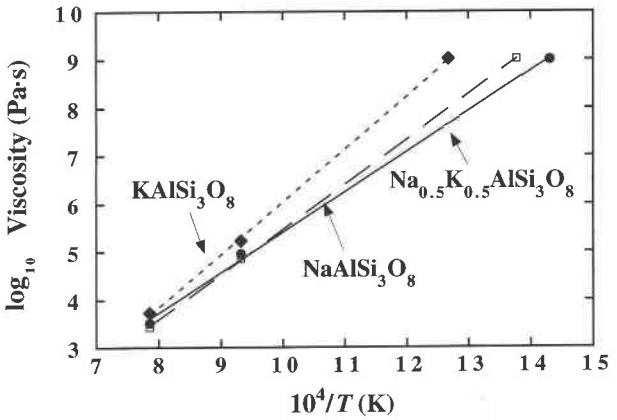

Fig. 5. A comparison of viscosity data derived from the calculation scheme of Shaw (1972) for higher temperature and the glass transition temperatures of the hydrous melts quenched in this study using the methods of Dingwell and Webb (1990). The good agreement indicates an Arrhenian temperature dependence of viscosity for the hydrous melts up to 10^9 Pa·s. These data are strong support for the validity of the present method for the determination of T_g (see text).

differential pressure. However, fluid inclusions from these samples always decrepitated prior to liquid-vapor homogenization when they were heated without being encapsulated in silica tubes. Thus, we conclude that the upper limit for the threshold of differential pressure required for decrepitation is <64 bars. We also note that inclusions from these samples remained intact under differential pressures of 2000 bars in the opposite sense (i.e., $P_{ex} > P_{int}$) for a brief period at temperatures as high as 200 °C. Returning to our hypothetical T_h = 280 °C fluid inclusion, if it homogenizes at 280 °C in the liquid phase (by expansion of the liquid, eliminating the vapor phase), the density is 0.75 g/cm³. During continuous heating above 280 °C, the pressure increases rapidly, at about 12 bars/°C, along the ρ = 0.75 isochore. Hence even a small amount of overheating can yield high internal pressures. These are compensated for by the liquid H_2O and steam sealed in the silica tube. As this internal pressure increases, the inclusions may stretch or decrepitate. Decrepitated, empty inclusions are easily recognizable and hence do not cause problems of measurement accuracy, but clearly decrepitation must be avoided for T_h measurement.

Results

Microthermometric data from all the samples measured are presented in Table 2 and Figure 3. The ranges in measured homogenization temperature are given for each sample. Glass transition temperatures for the binary $NaAlSi_3O_8$-$KAlSi_3O_8$ system, calculated from fluid-inclusion homogenization temperatures using volumetric data for pure H_2O from Keenan et al. (1964) and Burnham et al. (1969), are also shown in Figure 3. The mean values of the glass transition temperature range from 515–416 °C. The $KAlSi_3O_8$ glass has a significantly higher transition temperature than the albite glass. The H_2O contents of these H_2O saturated glasses, taken from the solubility study of Romano et al. (in preparation) are reported in Table 1, together with the compositions of the system. Here we emphasize that the compositions reported in Figure 3 are not truly binary, as the H_2O content varies from 6.0 wt% in albite melt to 5.1 wt% in orthoclase melt. The higher glass transition of orthoclase melt is consistent with the higher viscosity of the dry melt, as well as the lower H_2O content of the saturated melt. The composition dependence of the glass transition along this binary join shows a significant negative deviation from additivity. This deviation from additivity is a common feature of the transport properties of low-temperature, highly viscous, silicate melt binaries. Well-known examples of this effect are described in particular for the case of mixing of the alkalis under the term mixed-alkali effect (e.g., electrical conductivity: Isard, 1969; viscosity: Richet, 1984).

Dry vs. wet melts: T_g

We also measured the glass transition temperatures of the dry, starting-glass compositions for comparison. The measurements were performed by scanning push-rod dilatometry using methods described previously (Knoche et al., 1992). The peak temperatures of the expansivity curves yielded the glass transition temperatures that are presented in Table 3 and in Figure 4. Here again, both a higher glass transition temperature for the orthoclase composition as well as a negative deviation from additivity along the binary join are apparent. We can now see that the effect of H_2O on the glass transition temperature is enormous. The glass transition temperatures of the H_2O-saturated glasses are 370–460 °C below those of the dry glasses of equivalent composition. (The observation that the effective quench rates for the dilatometric experiments were considerably lower than the rapid quench of the hydrothermal glasses actually increases the difference between the T_g of dry and wet glasses by perhaps 30–40 °C.) This is, at least in part, a reflection of the efficiency

TABLE 4. Densities (g/cm³) of glasses in the $NaAlSi_3O_8$-$KAlSi_3O_8$ system

Glass	Dry (±0.002)	Wet* (±0.002)
K_{100}	2.359	2.306
$K_{90}Na_{10}$	2.364	2.312
$K_{70}Na_{30}$	2.370	2.317
$K_{50}Na_{50}$	2.373	2.320
$K_{30}Na_{70}$	2.373	2.322
$K_{10}Na_{90}$	2.373	2.310
Na_{100}	2.366	2.302

* Glasses saturated at $P = 2$ kbar and $T = 1100$ °C.

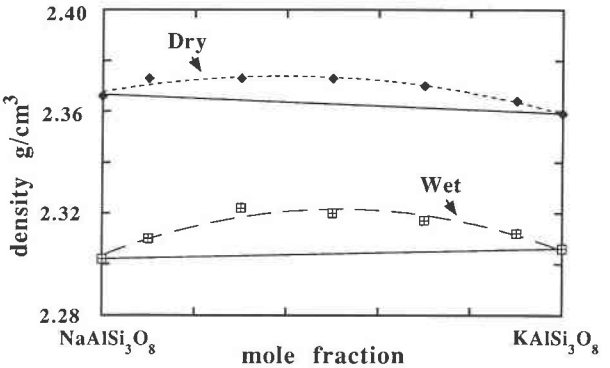

Fig. 6. Densities of quenched glasses measured using a Berman balance. The deviations from additivity can be attributed entirely to the effects of nonlinear variation in the glass transition temperature. These data are a source of information on the expansivity of dry and wet melts (see text).

of H_2O in reducing the volume relaxation time of the melts and is completely consistent with the drastic effect of H_2O on the shear viscosity (and shear relaxation time) of the melts (Shaw, 1963). The intrinsic effect of pressure on the relaxation time of feldspathic melts is estimated to be minor, on the basis of the glass transition measurements of Rosenhauer et al. (1979) and viscosity measurements of Kushiro (1978).

Viscosity

The quench rate during the preparation of hydrous glasses has been estimated at 200 °C/s. Using the relationship between quench rate and effective relaxation time available during the quench (Dingwell and Webb, 1990), together with the Maxwell relation between viscosity and shear relaxation time, we can calculate the viscosity that corresponds to the glass transition temperature that we have determined above. For a quench rate of $10^{2.3}$ °C/s we obtained a relaxation time of $10^{-1.7}$ (using a shear modulus of 25 GPa), and for such a relaxation time we obtained a viscosity of 10^9 Pa·s. The viscosity and temperature values can now be compared with the calculated viscosity-temperature relationship for each melt using the method of Shaw (1972). We can see from the presentation of this comparison in Figure 5 that the viscosity-temperature relationship predicted from the method of Shaw (1972), together with the value for viscosity provided by the glass transition, can be fitted for each sample within the errors associated with both using a linear regression. This means that the viscosity-temperature relationship of the H_2O-rich melts investigated in this study is Arrhenian, within error, over the investigated range. This result is somewhat unexpected, as the usual consequence of adding a depolymerizing agent to a polymerized composition is to make the viscosity-temperature relationship more strongly non-Arrhenian, that is more fragile in the sense of Angell (1984). It is possible, however, that the viscosity range over which the comparison of Figure 5 is being made is not large enough or does not extend to low enough temperature to observe the non-Arrhenian behavior. Nevertheless, the indication from the present comparison that the temperature dependence of the viscosity of H_2O-rich melts over this range of viscosity (up to 10^9 Pa·s) is Arrhenian is a significant result. If maintained for other melt compositions, this will greatly simplify the task of predicting low-temperature melt viscosities in silicic melts.

The comparison of Figure 5 has one other consequence. If some instability in the densities of our fluid inclusions had been a significant factor in determining the glass transition temperature, then the resulting decrease in density would be marked by an increase in the calculated glass transition temperature. All silicate melts indicate either constant or increasing activation energy of viscous flow with decreasing temperature. For the inclusion data of Figure 3 to have yielded higher glass-transition temperature data because of instability and yet agree with the estimates from Shaw's (1972) method (as is the case) would require that the true glass transition temperatures at lower temperature yield a decreasing activation energy of viscous flow with decreasing temperature—something that has never been observed. Thus the glass transition temperatures determined in this study, by virtue of the Arrhenian agreement with high-temperature calculated viscosities yielded the lowest possible, and therefore the true glass transition, temperature.

Expansivity

The densities of bubble-free glasses quenched from the same conditions at the same rates have been determined for the dry and wet joins. These data are presented in Table 4 and Figure 6. The deviation from additivity is evident in both cases. If we assume a linear volume composition relation for these joins and similar expansivities for the glasses, and ignore, in the case of the wet melts, the slight composition dependence of the H_2O solubility, then we can estimate the expansivity of the melt from the deviation of density from additivity. To do this we divide the deviation from additivity in the density by that of the glass transition temperature. The result yields values of expansivity, which are presented in Figure 7. The expansivity of the wet melts can be seen to be higher than those estimated for the dry melts.

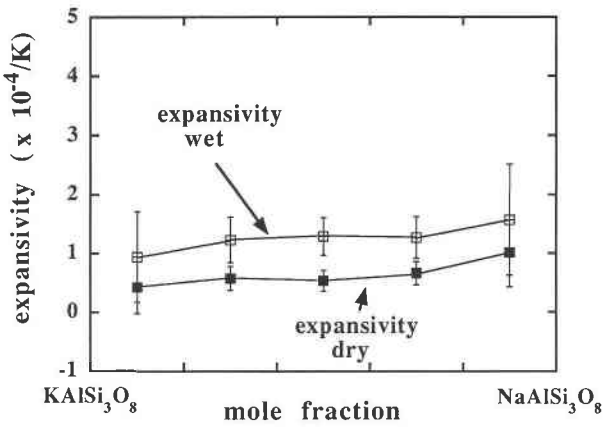

Fig. 7. The calculated expansivities for dry and wet melts on the albite-orthoclase join using the data from Figs. 3, 4, and 6 on the deviations from additivity of T_g and density, together with the assumption of linear volume-composition relations on the albite-orthoclase join (see text).

Conclusions

We wish to emphasize that the quantification of the thermal history of fluid inclusions quenched into silicate melts opens up many possibilities for the accurate determination of melt properties. The method is simple in principle, and the samples are easily synthesized. We have illustrated the possibility of determining the viscosity and expansivity with the method. Further possibilities include the study of the temperature dependence of melt structure by spectroscopic means. We are currently testing one example, the speciation of H_2O (Romano et al., in preparation). Another possibility is the determination of isoviscous conditions for melts with varying H_2O content but produced under similar conditions in equilibrium with a vapor phase diluted by CO_2.

Yet another possible application is the investigation of cooling rate dependence of inclusion data to evaluate macroscopic exchange of H_2O between melt and vapor with cooling. Holtz et al. (in preparation) have demonstrated that the temperature dependence of H_2O solubility can be either positive or negative; thus the kinetics of inclusion–host melt exchange could be complex. Further investigations of the behavior of inclusions during depressurization in the liquid state are also, in principle possible.

Acknowledgments

We thank Hubert Schulze for assistance with sample preparation and Detlef Krauße for analytical assistance, as well as I-Ming Chou for discussions and material assistance. This work has been supported by the Deutsche Forschungsgemeinschaft Gerhard-Hess-Programm (Di 431/3-1).

References cited

Angell, C.A. (1984) Strong and fragile liquids. In K.L. Ngai and G.B. Wright, Eds., Relaxation in complex systems, 345 p. Office of Naval Research and Technical Information Service, Arlington, Virginia.

Bagdassarov, N.Sh., Dingwell, D.B., and Webb, S.L. (1993) Effects of F, B and P on shear stress relaxation in haplogranitic melts. European Journal of Mineralogy, 3, 409–426.

Brandriss, M.E., and Stebbins, J.F. (1988) Effect of temperature on the structure of silicate liquids: 29Si NMR results. Geochimica et Cosmochimica Acta, 52, 2659–2669.

Burnham, C.W. (1963) Viscosity of a water-rich pegmatite. Special Paper Geological Society of America, 76, 26 p.

Burnham, C.W., and Davis, N.F. (1971) The role of water in silicate melts: I. *P-V-T* relations in the system $NaAlSi_3O_8$-H_2O to 1 Kilobar and 1100°C. American Journal of Science, 270, 54–79.

Burnham, C.W., Holloway, J.R., and Davis, N.F. (1969) Thermodynamic properties of water to 1000°C and 10,000 bars. The Geological Society of America Special Paper, 132, 96 p.

Carron, J.-P. (1969) Vue d'ensemble sur la rhéologie des magmas silicatés naturels. Bulletin de la Société française de Minéralogie et de Cristallographie, 92, 435–446.

Dingwell, D.B. (1990) Effects of structural relaxation on cationic tracer diffusion in silicate melts. Chemical Geology, 182, 209–216.

——— (1993) Experimental strategies for the investigation of low temperature properties in granitic and pegmatitic melts. Chemical Geology, 108, 19–30.

Dingwell, D.B., and Webb, S.L. (1989) Structural relaxation in silicate melts and non-newtonian melt rheology in geologic processes. Physics and Chemistry of Minerals, 16, 508–516.

——— (1990) Relaxation in silicate melts. European Journal of Mineralogy, 2, 427–449.

Eckert, H., Yesinowski, J.P., Stolper, E.M., Stanton, T.R., and Holloway, J. (1987) The state of water in rhyolitic glasses: A deuterium NMR study. Journal of Non-Crystalline Solids, 93, 93–114.

Fisher, R.V., and Schminke, H.-U. (1984) Pyroclastic rocks, 472 p. Springer-Verlag, Berlin.

Holtz, F., Behrens, H., Dingwell, D.B., and Taylor, R. (1992) Water solubility in aluminosilicate melts of haplogranitic composition at 2 kbar. Chemical Geology, 96, 289–302.

Holtz, F., Dingwell, D.B., and Behrens, H. (1993) The effects of fluorine, boron and phosphorus on the solubility of water in haplogranitic melts compared to natural melts. Contributions to Mineralogy and Petrology, 113, 502–523.

Ihinger, P. (1991) An experimental study of the interaction of water with granitic melt, 190 p. Ph.D. thesis, California Institute of Technology, Pasadena, California.

Isard, J.O. (1969) Mixed alkali effect in glass. Journal of Non-Crystalline Solids, 1, 235–261.

Keenan, J.H., Keyes, F.G., Hill, P.G., and Moore, J.G. (1964) Steam tables: Thermodynamic properties of water including vapor, liquid and solid phases, 156 p. Wiley Interscience, New York.

Knoche, R., Dingwell, D.B., and Webb, S.L. (1992) Temperature-dependent thermal expansivities of silicate melts: The system anorthite-diopside. Geochimica et Cosmochimica Acta, 56, 689–699.

Kohn, S.C., Dupree, R., and Smith, M.E. (1989) A multinuclear magnetic resonance study of the structure of hydrous albite glasses. Geochimica et Cosmochimica Acta, 53, 2925–2935.

Kushiro, I. (1978) Viscosity and structural changes of albite ($NaAlSi_3O_8$) melt at high pressures. Earth and Planetary Science Letters, 41, 87–90.

Leroy, J. (1978) The Margnac and Fanay uranium deposits of the La Crouzille district (western massive central, France): Geology and fluid inclusion studies. Economic Geology, 73, 1611–1634.

Martens, R.M., Rosenhauer, M., Büttner H., and von Gehlen, K. (1987) Heat capacity and kinetic parameters in the glass transformation interval of diopside, anorthite and albite glass. Chemical Geology, 62, 49–70.

Mysen, B.O., and Frantz, J.D. (1992) Raman spectroscopy of silicate melts at magmatic temperatures: Na_2O-SiO_2, K_2O-SiO_2 and Li_2O-SiO_2 binary compositions in the temperature range 25-1475°C. Chemical Geology, 96, 321–332.

Naumov, V.B., Balitskiy, V.S., and Khetchikov, L.N. (1966) Correlation of the temperatures of formation, homogenization, and decrepitation of gas-fluid inclusions. Akademiya Nauk SSSR Doklady, 171, 146–148.

Richet, P. (1984) Viscosity and configurational entropy of silicate melts. Geochimica et Cosmochimica Acta, 48, 471–484.

Richet, P., and Bottinga, Y. (1984) Anorthite, andesine, wollastonite, diopside, cordierite and pyrope: Thermodynamics of melting, glass transitions, and properties of the amorphous phases. Earth and Planetary Science Letters, 67, 415–432.

Roedder, E. (1965) Liquid CO_2 inclusions in olivine-bearing nodules and phenocrysts from basalts. American Mineralogist, 50, 1746–1782.

Rosenhauer, M., Scarfe, C.M., and Virgo, D. (1979) Pressure dependence of the glass transition in glasses of diopside, albite and sodium trisilicate composition. Carnegie Institution of Washington Year Book, 78, 556–559.

Sabatier, G. (1956) Influence de la teneur en eau sur la viscosité d'une rétinite, verres ayant la composition chimique d'un granite. Comptes Rendus, 242, 1340–1342.

Scherer, G.W. (1986) Relaxation in glass and composites, 331 p. Wiley, New York.

Shaw, H.R. (1963) Obsidian-H_2O viscosities at 1000 and 2000 bars in the temperature range 700 to 900°C. Journal of Geophysical Research, 68, 6337–6343.

Shaw, H.R. (1972) Viscosities of magmatic silicate liquids: An empirical method of prediction. American Journal of Science, 272, 870–889.

Silver, L., and Stolper, E.M. (1985) A thermodynamic model for hydrous silicate melts. Journal of Geology, 93, 161–178.

——— (1989) Water in albitic glass. Journal of Petrology, 30, 667–709.

Silver, L., Ihinger, P.D., and Stolper, E.M. (1990) The influence of bulk composition on the speciation of water in silicate glasses. Contributions to Mineralogy and Petrology, 104, 142–162.

Spera, F.J., Borgia, A., Strimple, J., and Feigenson, M. (1981) Rheology of melts and magmatic suspensions: I. Design and calibration of concentric cylinder viscometer with application to rhyolitic magma. Journal of Geophysical Research, 93, 10273–10294.

Stolper, E.M. (1982a) The speciation of water in silicate melts. Geochimica et Cosmochimica Acta, 46, 2609–2620.

——— (1982b) Water in silicate glasses: An infrared spectroscopic study. Contributions to Mineralogy and Petrology, 81, 1–17.

——— (1989) Temperature dependence of the speciation of water in rhyolitic melts and glasses. American Mineralogist, 74, 1247–1257.

Swanenberg, H.E.C. (1980) Fluid inclusions in high-grade metamorphic rocks from S.W. Norway. Geologica ultraiectina Univ Utrecht, 25, 147 p.

Taniguchi, H. (1981) Effects of water on the glass transition temperature of rhyolitic melt. Journal of the Japanese Association of Mineralogy, Petrology and Geochemistry, 76, 49–57.

Tool, A.Q., and Eichlin, C.G. (1931) Variations caused in the heating curves of glass by heat treatment. Journal of the American Ceramic Society, 14, 276–308.

Watson, E.B. (1981) Diffusion in magmas at depth in the earth: The effects of pressure and dissolved water. Earth and Planetary Science Letters, 52, 291–301.

Webb, S.L. (1992) Shear, volume, enthalpy and structural relaxation in silicate melts. Chemical Geology, 96, 449–457.

Webb, S.L., and Dingwell, D.B. (1990a) The onset of non-newtonian rheology of silicate melts: A fiber elongation study. Physics and Chemistry of Minerals, 17, 125–132.

——— (1990b) Non-newtonian rheology of igneous melts at high stresses and strain rates: Experimental results for rhyolite, andesite, basalt, and nephelinite. Journal of Geophysical Research, 95, 695–701.

Webb, S.L., Knoche, R., and Dingwell, D.B. (1992) Determination of silicate liquid thermal expansivity using dilatometry and calorimetry. European Journal of Mineralogy, 4, 95–104.

Werre, R.W., Jr., Bodnar, R.J., Bethke, P.M., and Barton, P.B., Jr. (1979) A novel gas-flow fluid inclusion heating/freezing stage. Geological Society of America Abstracts with Programs, 11, 539.

Zhang, Y., Stolper, E.M., and Wasserburg, G.J. (1990) Diffusion of water in rhyolitic glasses. Geochimica et Cosmochimica Acta, 55, 441–456.

Manuscript received November 16, 1993
Manuscript accepted July 8, 1994